Observation Wards and Control of the Transmission of COVID-19 in Wuhan

Juan Li [1,2,3*], Pei Yuan [1,3*], Jane Heffernan[1], Tingting Zheng[1,3,4], Nick Ogden[5], Beate Sander[6,7,8], Jun Li [1,3,9], Qi Li[1,3,10], Jacques Bélair[11], Jude Dzevela Kong[1], Elena Aruffo[1], Yi Tan[1,3], Zhen Jin[2], Yong Yu[12], Meng Fan[13], Jingan Cui[14], Zhidong Teng[4], Huaiping Zhu[1,3 †]

Affiliations:
[1] Center of Diseases Modeling (CDM), Department of Mathematics and Statistics, York University, Toronto, Canada
[2] Complex Systems Research Center, Shanxi University, Taiyuan, Shanxi, China
[3] Laboratory of Mathematical Parallel Systems (LAMPS), York University, Toronto, Canada
[4] College of Mathematics and System Science, Xinjiang University, Urumqi, Xinjiang, China
[5] Public Health Risk Sciences Division, National Microbiology Laboratory, Public Health Agency of Canada, Canada
[6] Toronto Health Economics and Technology Assessment (THETA) Collaborative, University Health Network, Toronto, Canada
[7] Dalla Lana School of Public Health, University of Toronto, Toronto, Canada
[8] Public Health Ontario, Toronto, Canada
[9] School of Mathematics and Statistics, Xidian University, Xi'an, Shaanxi, China
[10] Department of Mathematics, Shanghai Normal University, Shanghai, China
[11] Département de Mathématiques et de Statistique, Université de Montréal, Montréal, Québec, Canada
[12] School of Public Health and Management, Hubei University of Medicine, Shiyan, Hubei, China
[13] School of mathematics and Statistics, Northeast Normal University, Changchun, China
[14] Department of Mathematics, Beijing University of Civil Engineering and Architecture, Beijing, China

* Co-first authors made the same contributions.
† Corresponding Author: Email: huaiping@mathstat.yorku.ca
(Submitted: 8 April 2020 – Published online: 9 April 2020)

DISCLAIMER

RECOMMENDED CITATION

Li J, Yuan P, Heffernan J, Zheng T, Ogden N, Sander B, et al. Observation wards and control of the transmission of COVID-19 in Wuhan. [Preprint]. *Bull World Health Organ*. E-pub: 9 April 2020. doi: http://dx.doi.org/10.2471/BLT.20.258152

Abstract:

Objectives: The megacity of Wuhan was the epicenter of the COVID-19 pandemic. However, by intense public health countermeasures, the epidemic was successfully stopped in 70 days. In this paper, we explore the critical factors among many countermeasures taken by the city that resulted in the epidemic being extinguished.

Methods: This is a fact and data driven modeling study. Using the classified data on daily reported confirmed cases of COVID-19, we establish and employ compartmental models to mimic the transmission of the virus in Wuhan. The three phases models incorporate the number of hospital beds in both designated hospitals and observation wards, in particular the number of beds in group observation wards for people with mild symptoms.

Findings: Our findings indicate that while designated hospitals saved the lives of the severely infected, it was a large number of observation wards, and thus, the extra hospital bed capacity, that helped slow down and eventually stop the epidemic of COVID-19 in Wuhan. Using our models, we assess the Wuhan city lockdown strategy and find that it was indeed a successful strategy to curb the spread of the virus.

Conclusion: Given the current global pandemic situation of COVID-19, this study suggests that, increasing the hospital bed capacity, especially the observation wards to group isolate the people with mild symptoms within an affected region could be key to curbing and eventually stop the outbreak in communities where effective household isolation is not possible.

Keywords: *COVID-19, Observation Wards, Hospital beds, Healthcare personnel, lockdown, control, isolation, transmission dynamics*

1. Introduction

Wuhan is a megacity, ranked the 42nd largest city in the world with an estimated population of 10 million. To control the transmission of COVID-19, Wuhan initiated a lockdown on January 23, 2020[1]. As an extraordinary measure, the city was quarantined and turned into an isolation ward[2].

In order to alleviate the massive shortage of doctors and medical resources, medical teams and materials were dispatched in batches to Wuhan from other parts of the country[3]. A large number of designated hospitals (DHs) were quickly organized, including building of new hospitals, to increase the capacity for accepting daily tested confirmed cases[4]. Among the collective efforts, the most remarkable campaign was in the building of Huoshenshan Hospital on January 23. Within 10 days (on February 2) the first batch of 1000 hospital beds were opened to take in confirmed cases. On January 25 the building of Leishenshan Hospital was initiated, and this added another 1500 new beds on February 8[5]. Yet, the epidemic situation continued, with the number of confirmed cases continuing to increase even though quarantine and social distancing policies were strictly enforced[6]. The situation did not improve at all until the open up of observation wards (OW) on February 5 which changed the stalemate situation in battling to curb the epidemic of the virus.

OWs were established for group isolating people with mild symptoms, a non-pharmaceutical measure to contain the transmission of the virus. The introduction of these OWs effectively

changed the family-based household quarantine into a massive group isolation[7]. As stated in the World Health Organization (WHO)-China joint mission report[8] that these measures to contain the COVID-19 virus quickly reversed the escalating situation which provides vital lessons for the global response.

To attain effective control, the Chinese government, in collaboration with the local government of Wuhan, decided to apply an intervention policy that move all patients together, teaming up all experts and doctors (healthcare personnel, HCP), centralizing all resources (aiming at improving treatment and care) and reducing the rate of new infections (moving infected people away from susceptible family members) and mortality[9]. In order to implement these policies, on February 3, Hubei province and the Wuhan City headquarters of epidemic prevention and control decided to treat patients by level of infection, and started to build OWs. Mildly affected patients were admitted into OWs, and DHs focused on the treatment of severe and critically infected patients[10]. Wuhan continued to build more and more OWs with increased sizes and by the middle of February, the numbers of daily new confirmed cases in HCP and the rest of the population started to slow down (Fig. 1).

Though the social distancing and quarantine strategies were strictly forced after the lockdown, Fig. 1 shows that DHs, while essential to the treatment of severely affected patients to save lives, which is the first priority during an outbreak, did not help to decrease the number of new infections. The continual effort in the building of OWs and patient isolation from susceptible family members, however, coincided with a dramatic decrease in infections, and is therefore likely a key policy to the success of the Wuhan pandemic control efforts.

While the hospital beds in both DHs and OWs, and having sufficient HCPs as well, were likely important in minimizing the spread of the virus in the city, it was recognized that the frontline HCPs in close contact with the infected and infectious patients had a much higher risk of infection and impacted transmission. According to a report from the COVID-19 epidemiological investigation team of emergency response mechanisms of the China CDC[11], in the period between the start of the outbreak and February 11, a total of 3019 HCPs were infected, and 5 died.

In this paper, we employ compartmental models to mimic the transmission of the virus in Wuhan and study how the megacity lockdown policy controlled the spread of the virus. There have been a number of previous dynamical modeling efforts on the spread of COVID-19 virus in Wuhan[12-15]. These models, however, have not considered the roles of both the addition of new functional hospital beds and the HCPs (reflection of public health resources and hospitalization ratio). The building and addition of new hospital beds (with additional HCPs) went through multiple stages, and our models incorporate these steps.

Our models are built on the classical SEIR compartmental framework. We divide the population into three categories: Wuhan general population, HCPs in DHs, and HCPs in OWs. The models are informed by demographic and clinical data, as well as the limited data on the number of hospital beds in DHs and OWs, and HCPs. We compute the reproduction number to assess the risk of HCP infection and that of the general public. We also estimate the hospital bed ratio (per 1,000 people) essential to control the infectious diseases in the model simulations.

While this paper was in preparation, the novel coronavirus COVID-19 quickly spread around the world. On March 11, the WHO declared the coronavirus outbreak a global pandemic[16]. In response to this declaration other countries, including Italy, Spain, the USA, and Canada started to implement isolation and quarantine measures to combat the virus[17-20]. Therefore, this study aims to supply valuable advice to policy makers regarding possible strategies to combat COVID-19 by

considering the use of increasing hospital bed capacity to enhance the efficiency of isolation of cases where home isolation is likely to be inefficient.

2. Data and Materials

The transmission of COVID-19 in Wuhan led to 50,003 infections and 2469 dead as of March 15, 2020[21]. We obtained data of the daily reported new confirmed cases, recovered cases and infection deaths in Wuhan from Jan 23 to March 17, 2020 from the official website of the Wuhan Municipal Health Commission (WMHC)[22]. We note that in the early days of the Wuhan outbreak, especially after the city was put in lockdown, testing resources (and HCPs) were limited. The data is therefore affected by testing wait times. There is a time lag from the date of symptom onset to the reporting date, and therefore, the number of reported confirmed cases in the data is not the actual number of COVID-19 infections in Wuhan on a specific day. In addition, the diagnostic criteria for COVID-19 were updated five times. As shown in Figure 1, the newly confirmed cases surged dramatically on Feb 13, 2020, reaching about 12000 new infections: this sudden jump can be attributed to a change in test standards in the 5th edition of the "COVID-19 Guideline"[23] released from the Chinese Government. As this change improved test efficiency, we use data only from February 12 onwards for data fitting.

It is recognized that the crucial factor that brought disease spread in Wuhan to an end was the increased in hospital and HCP resources. Hospitals and hospital beds, however, are where HCPs come into contact with infected people seeking diagnosis and treatment. We treat HCPs separately from the general public so as to track infections in this important healthcare resource.

Using the available published literature, we extracted data about infected HCPs in Wuhan, in Hubei province (except Wuhan), and the entire country[11,24,25] We then calculated the daily infection of HCPs in Wuhan from January 23 to February 11, 2020. The data show that at the early stage when the lockdown started, more HCPs were infected, due to the limited hospital and diagnosis capacity to aid an overwhelming number of patients (Fig. 1). This situation started to improve in mid-February when a large number of hospital beds were added through the building of OWs used to group quarantine and treat mild cases. In late February, no further new beds were needed to curb the spread of COVID-19 (Fig. 1).

HCPs and the number of hospital beds (in DHs and OWs) are closely related quantities that both can be used to measure control strategy efficacy. DH and OW bed capacity were estimated from hospital diagnoses data included in public reports from the Wuhan COVID-19 Epidemic Prevention and Control Headquarters. We then considered the role of HCPs and the HCP to DH and OW bed ratio over three different stages of the epidemic.

Denote $by\ T_0$ the date when the lockdown started (January 23), T_1 the date when the first bed in OWs opened to quarantine individuals (February 5), and T_2 the date when no new beds were built for OWs and more beds in OWs became available (February 22). We then define Phase I to be the time period from T_0 to T_1, Phase II the time period from T_1 to T_2, and Phase III the time period from T_2 to the end of the epidemic.

In each phase, the transmission of the virus changes due to the increasing number of DH and/or OW hospital beds. We denote $B_1(t)$ as the total number of DH beds on day t. If $b_1(t)$ is the number of newly built beds on day t, then

$$B_1(t) = B_1(T_0) + \int_{T_0}^{t} b_1(s)ds,\ t \geq T_0.$$

For OWs, we similarly define $B_2(t)$, the total number of OW beds on day t as

$$B_2(t) = \int_{T_1}^{t} b_2(s)ds,\ t \geq T_1$$

where $b_2(t)$is the number of newly built OW beds on day t.

In a standard DH or OW, the ratio of beds to HCP is usually fixed to guarantee efficacy. We use k_1 and k_2 to denote these ratios in DHs and OWs respectively. With information mainly from WMHC[27], news report[26,28], we calculate to find $k_1 = 2.486$ and k_2= 1.107. Therefore, the total number of HCPs in DHs and OWs can be determined.

With the construction of DHs and OWs, the number of hospital beds in Wuhan increased. The number of beds available is another important quantity that can be used to monitor epidemic progression and severity. Define $V_1(t)$ and $V_2(t)$ as the number of available DH and OW beds on day t, respectively. Fig. 2 shows that $V_1(t)$ and $V_2(t)$ started to increase on February 15th. It also shows that the accumulated total number of new confirmed cases started to decrease on February 22nd. We therefore do not count the extra beds built after February 22, 2020 even though the plan to build more OWs continued. We thus determine $B_2(22) = 13348$ as the limit of $B_2(t)$. Additionally, we define the end date of COVID-19 in Wuhan to coincide with the date that satisfies $B_i(t) = V_i(t), i = 1,2$ when all beds in DHs and OWs are available.

Fig. 2(a) shows the cumulative number of new beds in DHs (from January 23 to February 25) and OWs (from January 23 to February 22). We note that the daily number of new beds reported were not the actual number opened, and all beds opened were on a day to day basis [29-31]. We use the moving average method to smooth the cumulative number of beds to calculate the daily number of new beds put into use. The raw and processed data sets are shown in Fig. 2 (b) and (c).

3. Transmission models in three Phases

We make the following assumptions when modeling the transmission of the virus in each of the three phases described above:

- HCPs will be admitted if symptoms occur, and will be given priority to use hospital beds. In Phase I, confirmed HCPs will be admitted to the DHs. After Phase I, the HCPs with mild symptoms will be admitted to OWs with priority.
- Subclinical infected cases will recover from the infection and will not be re-infected[32].
- We ignore natural birth and mortality demographics of the population.
- All individuals exposed to the virus have the same probability of infection.
- HCPs who are asymptomatically infected still work in the hospitals.
- We neglect any possible transmission between non-HCPs not admitted in the hospital and HCPs.

3.1 Modeling for Phase I: T_0 (January 23) to T_1 (February 5)

The Phase I model is shown in Fig. 3. For non-HCPs, we classify the general population into the following groups: Susceptible ($S_w(t)$), Exposed ($E_w(t)$), Asymptomatic (subclinical) infection that will never show symptoms($A_w(t)$), Infected with no symptoms that will progress to the symptomatic classes, including Infectious but no symptoms ($I_{w1}(t)$) and Infected with symptoms ($I_{w2}(t)$), and Recovered ($R_w(t)$). It is assumed that severely infected individuals are admitted to DHs, and enter the $I_{wB_1}(t)$ class, after which they recover to $R_h(t)$ (the class of all those who recovered from the infection at the DHs), or die.

We subdivide the HCP population in DHs into similarly defined classes: $S_h(t)$, $E_h(t)$, $A_h(t)$, and $I_{h1}(t)$. It is assumed that infected symptomatic HCPs are immediately accepted into the $I_{wB_1}(t)$

class, and are provided beds in DHs with priority. All recovered non-HCPs and HCPs that are admitted in DHs recover to the $R_h(t)$ class or die.

Model equations for Non-HCPs in Wuhan:

$$\begin{cases} S_w' = -\beta_{w1} S_w (A_w + I_{w1}) - \beta_{w2} S_w I_{w2}, \\ E_w' = \beta_{w1} S_w (A_w + I_{w1}) + \beta_{w2} S_w I_{w2} - \frac{1}{\tau_1} E_w, \\ A_w' = (1-a)\frac{1}{\tau_1} E_w - \gamma_a A_w, \\ I_{w1}' = a\frac{1}{\tau_1} E_w - \frac{1}{\tau_2} I_{w1}, \\ I_{w2}' = \frac{1}{\tau_2} I_{w1} - L_1(V_1(t), I_{w2}) - \gamma_2 I_{w2} - d_w I_{w2}, \\ R_w' = \gamma_a A_w + \gamma_2 I_{w2}. \end{cases}$$

Model equations for HCPs in DHs:

$$\begin{cases} S_h' = \left(b_1(t)k_1 + \frac{1}{\tau_2} I_{h1}\right) - \beta_{\mathrm{h}} \left(S_h + b_1(t)k_1 + \frac{1}{\tau_2} I_{h1}\right) I_{wB_1} - \beta_{h1} \left(S_h + b_1(t)k_1 + \frac{1}{\tau_2} I_{h1}\right)(A_h + I_{h1}), \\ E_h' = \beta_{\mathrm{h}} \left(S_h + b_1(t)k_1 + \frac{1}{\tau_2} I_{h1}\right) I_{wB_1} + \beta_{h1} \left(S_h + b_1(t)k_1 + \frac{1}{\tau_2} I_{h1}\right)(A_h + I_{h1}) - \frac{1}{\tau_1} E_h, \\ A_h' = (1-a)\frac{1}{\tau_1} E_h - \gamma_a A_h, \\ I_{h1}' = a\frac{1}{\tau_1} E_h - \frac{1}{\tau_2} I_{h1}, \\ R_h' = \gamma_a A_h + \gamma I_{wB_1}, \\ I_{wB_1}' = L_1(V_1(t), I_{w2}) + \frac{1}{\tau_2} I_{h1} - d I_{wB_1} - \gamma I_{wB_1}, \end{cases}$$

where $L_1(V_1(t), I_{w2})$ is the number of non-HCPs including severe and mild cases accepted into DHs on day t, which depends on the number of available beds $V_1(t)$ and the number of severely infected patients that need beds on day t. During Phase I, the number of beds were not sufficient for the severely infected demand. Here $L_1(V_1(t), I_{w2})$ is defined to be the sum of the number of available beds $V_1(t)$ (due to the newly built beds $b_1(t)$) and the number of admitted patients that exit the DH (through death or recovery)), minus the number of newly infected HCPs:

$$L(V_1(t), I_{w2}) = V_1(t) - \tfrac{1}{\tau_2} I_{h1} = b_1(t) + (\gamma + d) I_{wB_1}(t) - \tfrac{1}{\tau_2} I_{h1}.$$

If we let $X_w(t) = \left(S_w(t),\ E_w(t),\ A_w(t),\ I_{w1}(t),\ I_{w2}(t),\ R_w(t)\right)$ and $X_h(t) = (\ S_h(t),\ E_h(t),\ A_h(t),\ I_{h1}(t),\ R_h(t),\ I_{wB_1}(t))$, then the initial value for all model populations for the first phase model is given by $X_w(T_0) = (S_w^*,\ E_w^*,\ A_w^*,\ I_{w1}^*,\ I_{w2}^*,\ R_w^*)$, and $X_h(T_0) = (S_h^*, 0, 0, 0, R_h^*, I_{wB_1}^*)$.

3.2 Modeling Phase II from T_1 (February 5) to T_2 (February 22)

In Phase II we account for the increased bed capacity through the building of OWs. These beds were used to change the family-based household quarantine into a massive group quarantine. Eventually, on February 22, the situation started to change, and more and more occupied beds became empty in OWs.

Here we assume the same model structure for the $X_w(t)$ and $X_h(t)$ populations as in Phase I. We also add a new class of OW HCPs, that are subdivided into $S_g(t)$, $E_g(t)$, $A_g(t)$, and $I_{g1}(t)$

classes. The non-HCPs that get admitted in the OWs fall into a class we denote as $I_{wB_2}(t)$. It is assumed that infected HCPs in OWs with mild symptoms are immediately accepted into the class $I_{wB_2}(t)$. It is also assumed that non-HCPs are admitted into OWs and DHs, depending on their symptoms and on the number of beds of each type that are given to HCPs admitted to the OWs and DHs. We note that $I_{wB_2}(t)$ cases can recover or be admitted to DHs as their symptoms become more severe. We further note that all $I_{wB_2}(t)$ cases that recover move to the $R_g$class, and that DH patients that are on the mend remain in the DH facilities (they do not move to the OWs). A flow diagram for Phase II (extended from the flow diagram from Phase I) is presented in Fig. 4.

Model equations for Non-HCPs in Wuhan:

$$\begin{cases} S_w' = -\beta_{w1} S_w (A_w + I_{w1}) - \beta_{w2} S_w I_{w2}, \\ E_w' = \beta_{w1} S_w (A_w + I_{w1}) + \beta_{w2} S_w I_{w2} - \frac{1}{\tau_1} E_w, \\ A_w' = (1-a)\frac{1}{\tau_1} E_w - \gamma_a A_w, \\ I_{w1}' = a\frac{1}{\tau_1} E_w - \frac{1}{\tau_2} I_{w1}, \\ I_{w2}' = \frac{1}{\tau_2} I_{w1} - L_1(V_1(t), I_{w2}) - L_2(V_2(t), I_{w2}) - \gamma_2 I_{w2}, \\ R_w' = \gamma_a A_w + \gamma_2 I_{w2}. \end{cases}$$

Model equations for HCPs in DHs:

$$\begin{cases} S_h' = \left(b_1(t)k_1 + \frac{1}{\tau_2} I_{h1}\right) - \beta_{\mathrm{h}} \left(S_h + b_1(t)k_1 + \frac{1}{\tau_2} I_{h1}\right) I_{wB_1} - \beta_{h1} \left(S_h + b_1(t)k_1 + \frac{1}{\tau_2} I_{h1}\right)(A_h + I_{h1}), \\ E_h' = \beta_{\mathrm{h}} \left(S_h + b_1(t)k_1 + \frac{1}{\tau_2} I_{h1}\right) I_{wB_1} + \beta_{h1} \left(S_h + b_1(t)k_1 + \frac{1}{\tau_2} I_{h1}\right)(A_h + I_{h1}) - \frac{1}{\tau_1} E_h, \\ A_h' = (1-a)\frac{1}{\tau_1} E_h - \gamma_a A_h, \\ I_{h1}' = a\frac{1}{\tau_1} E_h - \frac{1}{\tau_2} I_{h1}, \\ R_h' = \gamma_a A_h + \gamma I_{wB_1}, \\ I_{wB_1}' = L_1(V_1(t), I_{w2}) + \frac{1}{\tau_2} I_{h1} - d I_{wB_1} - \gamma I_{wB_1} + \sigma_1 I_{wB_2}. \end{cases}$$

Model equations for HCPs in OWs:

$$\begin{cases} S_g' = \left(b_2(t)k_2 + \frac{1}{\tau_2} I_{g1}\right) - \beta_g \left(S_g + b_2(t)k_2 + \frac{1}{\tau_2} I_{g1}\right) I_{wB_2} - \beta_{g1} \left(S_g + b_2(t)k_2 + \frac{1}{\tau_2} I_{g1}\right)(A_g + I_{g1}), \\ E_g' = \beta_g \left(S_g + b_2(t)k_2 + \frac{1}{\tau_2} I_{g1}\right) I_{wB_2} + \beta_{g1} \left(S_g + b_2(t)k_2 + \frac{1}{\tau_2} I_{g1}\right)(A_g + I_{g1}) - \frac{1}{\tau_1} E_g, \\ A_g' = (1-a)\frac{1}{\tau_1} E_g - \gamma_a A_g, \\ I_{g1}' = a\frac{1}{\tau_1} E_g - \frac{1}{\tau_2} I_{g1}, \\ R_g' = \gamma_a A_g + \gamma_m I_{wB_2}, \\ I_{wB_2}' = L_2(V_2(t), I_{w2}) + \frac{1}{\tau_2} I_{g1} - \gamma_m I_{w2} - \sigma_1 I_{wB_2}, \end{cases}$$

where $L_1(V_1(t), I_{w2})$ and $L_2(V_2(t), I_{w2})$ are given by

$$L_1(V_1(t), I_{w2}) = V_1(t) - \sigma_1 I_{wB_2} - \tfrac{1}{\tau_2} I_{h1} = b_1(t) + (\gamma + d) I_{wB_1}(t) - \sigma_1 I_{wB_2} - \tfrac{1}{\tau_2} I_{h1},$$

$$L_2(V_2(t), I_{w2}) = V_2(t) - \tfrac{1}{\tau_2} I_{g1} = b_2(t) + (\gamma_m + \sigma_1) I_{wB_2}(t) - \tfrac{1}{\tau_2} I_{g1}.$$

Here $L_2(V_2(t), I_{w2})$ is determined by the number of available beds $V_2(t)$ for non-HCPs in OWs and the number of mildly infected individuals $I_{w2}(t)$ who need the beds on day t.

If we let $X_w(t) = (S_w(t), E_w(t),\ A_w(t), I_{w1}(t),\ I_{w2}(t),\ R_w(t))$, $X_h(t) = (\ S_h(t),\ E_h(t),\ A_h(t),\ I_{h1}(t),\ R_h(t),\ I_{wB_1}(t))$, and $X_g(t) = (S_g(t), E_g(t), A_g(t), I_{g1}(t), R_g(t), I_{wB_2}(t))$, then the initial conditions for the second phase can be written as $(X_w(T_1), X_h(T_1), X_g(T_1))$, where $X_w(T_1), X_h(T_1)$ and $X_g(T_1)$ are determined by the terminating conditions from Phase I, and $X_w(T_1) = \ (S_w(T_1),\ E_w(T_1),\ A_w(T_1),\ I_{w1}(T_1),\ I_{w2}(T_1),\ R_w(T_1)\ )$, and $X_h(T_1) = \ (S_h(T_1),\ \ E_h(T_1),\ A_h(T_1),\ I_{h1}(T_1), R_h(T_1),\ I_{wB_1}(T_1)\ )$, and $X_g(T_1) = (S_g(T_1),\ E_g(T_1),\ A_g(T_1),\ I_{g1}(T_1),\ R_g(T_1),\ I_{wB_2}(T_1))$.

3.3 Modeling Phase III after T_2 (February 22)

In Phase III, due to the stabilizing number of available beds, all confirmed mildly infected and severely infected patients through contacting tracing and testing can be accepted into DHs and OWs immediately. We therefore assume that there is no I_{w2} in this phase. Again, we assume that DH patients with ameliorating symptoms in DHs will not move to OWs. With the flow diagram in Fig. 5, we have the following model:

Model equations for Non-PCPs:

$$\begin{cases} S_w' = -\beta_{w1} S_w (A_w + I_{w1}), \\ E_w' = \beta_{w1} S_w (A_w + I_{w1}) - \frac{1}{\tau_1} E_w, \\ A_w' = (1-a)\frac{1}{\tau_1} E_w - \gamma_a A_w, \\ I_{w1}' = a\frac{1}{\tau_1} E_w - \frac{1}{\tau_2} I_{w1}, \\ R_w' = \gamma_a A_w. \end{cases}$$

Model equations for HCPs in DHs:

$$\begin{cases} S_h' = -\beta_{\mathrm{h}} S_h I_{wB_1} - \beta_{h1} S_h (A_h + I_{h1}), \\ E_h' = \beta_{\mathrm{h}} S_h I_{wB_1} + \beta_{h1} S_h (A_h + I_{h1}) - \dfrac{1}{\tau_1} E_h, \\ A_h' = (1-a)\dfrac{1}{\tau_1} E_h - \gamma_a A_h, \\ I_{h1}' = a\dfrac{1}{\tau_1} E_h - \dfrac{1}{\tau_2} I_{h1}, \\ R_h' = \gamma_a A_h + \gamma I_{wB_1}, \\ I_{wB_1}' = \mathrm{p}\dfrac{1}{\tau_2} I_{w1} + \dfrac{1}{\tau_2} I_{h1} - d I_{wB_1} - \gamma I_{wB_1} + \sigma_1 I_{wB_2}. \end{cases}$$

Model equations for HCPs in OWs:

$$\begin{cases} S_g' = -\beta_{\mathrm{g}} S_g I_{wB_2} - \beta_{g1} S_g \left(A_g + I_{g1}\right), \\ E_g' = \beta_{\mathrm{g}} S_g I_{wB_2} + \beta_{g1} S_g \left(A_g + I_{g1}\right) - \dfrac{1}{\tau_1} E_g, \\ A_g' = (1-a)\dfrac{1}{\tau_1} E_g - \gamma_a A_g, \\ I_{g1}' = a\dfrac{1}{\tau_1} E_g - \dfrac{1}{\tau_2} I_{g1}, \\ R_g' = \gamma_a A_g + \gamma_m I_{wB_2}, \\ I_{wB_2}' = (1-\mathrm{p})\dfrac{1}{\tau_2} I_{w1} + \dfrac{1}{\tau_2} I_{g1} - \gamma_m I_{wB_2} - \sigma_1 I_{wB_2}. \end{cases}$$

Here, $V_1(t)$ and $V_2(t)$ satisfy

$$V_1(t) = B_1(t) - I_{wB_1} + \sigma_1 I_{wB_2} + \tfrac{1}{\tau_2} I_{h1}.$$

$$V_2(t) = B_2(t) - I_{wB_2} + \tfrac{1}{\tau_2} I_{w1} + \tfrac{1}{\tau_2} I_{g1}.$$

If we let $X_w(t) = (S_w(t), E_w(t), A_w(t), I_{w1}(t), R_w(t))$, $X_h(t) = (S_h(t),\ E_h(t), A_h(t),\ I_{h1}(t), R_h(t), I_{wB_1}(t))$, and $X_g(t) = (S_g(t), E_g(t), A_g(t), I_{g1}(t), R_g(t), I_{wB_2}(t))$, then the initial conditions for Phase III can be written as $(X_w(T_2), X_h(T_2), X_g(T_2))$, where $X_w(T_2), X_h(T_2)$ and $X_g(T_2)$ are determined by conditions in Phase II with $X_w(T_2) = (S_w\ (T_2),\ E_w\ (T_2),\ A_w(T_2),\ I_{w1}(T_2),\ R_w(T_2))$, $X_h(T_2) = (S_h(T_2),\ E_h(T_2), A_h(T_2), I_{h1}(T_2),\ R_h(T_2), I_{wB_1}(T_2))$, and $X_g(T_2) = (S_g(T_2), E_g(T_2), A_g(T_2), I_{g1}(T_2), R_g(T_2), I_{wB_2}(T_2))$.

We summarize the variables and parameters in the models for the three phases in Tables 1 and 2.

4. Basic reproduction number and risk assessment in DHs and OWs

Due to the continuous input of beds and HCPs in hospitals, there is no disease-free equilibrium (DFE) in the model for Phases I and II. In Phase III, there is no more input of beds and HCPs, and a DFE can be calculated: $E_0 = (S_{w0},\ 0,\ 0,\ 0,\ R_{w0},\ S_{h0},\ 0,\ 0,\ 0,\ R_{h0},\ 0,\ S_{g0},\ 0,\ 0,\ 0,\ R_{g0},$

$0)$, where $S_{w0},\ S_{h0},\ S_{g0},\ R_{w0}, R_{h0}$ and R_{g0} are any positive integers representing their numbers at a disease free state.

Using the next-generation matrix method[33], we calculate the basic reproduction number for Phase III, R_0 (the average number of the infected individuals by a single infectious individual in the whole susceptible population) as $R_0 = max\{R_{0w}, R_{0h}, R_{0g}\}$, where $R_{0w} = S_{w0}\beta_{w1}\left(a\tau_2 + \frac{1-a}{\gamma_a}\right)$, $R_{0h} = S_{h0}\left(\frac{a\beta_h}{d+\gamma} + \beta_{h1}\left(a\tau_2 + \frac{1-a}{\gamma_a}\right)\right)$, and $R_{0g} = S_{g0}\left(\frac{a\beta_g}{\gamma_m+\sigma_1} + \beta_{g1}\left(a\tau_2 + \frac{1-a}{\gamma_a}\right)\right)$. Here R_{0w}, R_{0h} and R_{0g} are the basic reproduction numbers measuring the transmission power of the virus in the non-HCP, DH HCP, and OW HCP sub-populations, respectively.

As the number of DH and OW beds increased, higher hospitalization and isolation rates could be achieved, thereby leading to a decrease in the infection risk of susceptibles in all sub-populations. Using ideas from[34-38] and based on the formulae for the basic reproduction numbers R_{0w}, R_{0h} and R_{0g} we define the instantaneous risk index as $R_0(t) = \{R_{0w}(t), R_{0h}(t), R_{0g}(t)\}$ with $R_{0w}(t) = \beta_{w1}(S_w(t)\left(a\tau_2 + \frac{1-a}{\gamma_a}\right) + \beta_{w2}S_w(t)\frac{a}{\gamma_2+d_w(t)+\eta(t)}$, $T_0 \le T < T_2$,

$R_{0h}(t) = \beta_h(\ S_h\ (t) +\ b_1(t)k_1\ )\ \frac{a}{d+\gamma}\ +\ \beta_{h1}(S_h(t) + b_1(t)k_1)\left(a\tau_2 + \frac{1-a}{\gamma_a}\right)$, $T_0 \le T < T_2$, and $R_{0g}(t) = \beta_g\left(S_g(t) + b_2(t)k_2\right)\frac{a}{\sigma_1+\gamma_m} + \beta_{g1}\left(S_g(t) + b_2(t)k_2\right)\left(a\tau_2 + \frac{1-a}{\gamma_a}\right)$, $T_0 \le T < T_2$, reflecting the risk of an of infection in the non-HCP, DH HCP, and OW HCP sub-populations. Here

$$d_w(t) = \begin{cases} d_w, & T_0 \le t \le T_1, \\ 0, & t > T_1. \end{cases}$$

In particular, we introduce the hospitalization ratio in different phases as

$$\eta(t) = \begin{cases} \dfrac{L_1(V_1(t), I_{w2})}{\frac{1}{\tau_2} I_{w1}(t)}, & T_0 \le t \le T_1, \\ \dfrac{L_1(V_1(t), I_{w2}) + L_2(V_2(t), I_{w2})}{\frac{1}{\tau_2} I_{w1}(t)}, & t > T_1. \end{cases}$$

Since there is no $I_{w2}(t)$ compartment in Phase III, $\beta_{w2} = 0$. Therefore, $R_0(t) \to R_0\ as\ t \to T_2$. Using the estimated parameters, we calculate and explain how the increasing number of beds reduced the infection risk of the sub-populations, and eventually led to the halt of the epidemic.

5. Results

Using the data from Wuhan, we first present simulations of our model for each phase of the epidemic. We then quantify the impact of the HCPs and newly built hospital beds on the epidemic outcome, and discuss how crucial the timing and implementation of these resources were for infection mitigation.

5.1 Parameter estimation and simulation for the three phases in Wuhan

Using the data described in Section 2, we set the initial values and some of the parameters for each phase in the model. In Phase I, there were no OWs. Hence on the day T_0, the initial values of the

six state variables related to OWs were set to zero (see Table 1). We estimate the initial values for the 6 non-HCP state variables and the 14 unknown parameters (infection rate, recovery rate, mortality rate and proportion of symptomatic infection in each class) using Bayesian methods. Prior distributions for the model parameters were assumed to be multivariate Gaussian. The estimated value of the parameters and initial states were determined as the mean of the posterior distributions, which were obtained using Markov Chain Monte Carlo (MCMC) methods, employing the adaptive Metropolis-Hasting algorithm with 150,000 iterations and a 90,000 iteration burn-in reference[39]. Chain convergence was assessed by the Geweke statistic. All Geweke values were determined to be greater than 0.9, indicating satisfactory chain convergence.

Combining the number of new DH beds (January 23-February 25) and the number of OW beds (February 5-22) per day, we fit our model to the recorded data on the cumulative number of confirmed cases, recovered cases and deaths from January 23 to March 17, and the cumulative number of HCP confirmed cases from January 23 to February 11 in Wuhan. The estimated parameter values and their highest density intervals are shown in Tables 1 and 2. The results show that the model fits very well, the Normalized Mean Square Error (NMSE) = 0.97.

The data fitting and simulation results are presented in Fig. 6. The results of our parameter estimation indicate that 0.9530% (95% CI: 0.9502, 0.9560) of exposed cases progressed to symptomatic infections. Therefore, 4.7% (95% CI: 4.4%, 4.98%) of exposed cases progressed to subclinical infections. This is higher than the previously reported value of 1.2%[11].

Model simulation results show that the peak value of the outbreak is 39771 (95% CI: 39727, 39827), and that it occurred on February 21. Results also show that the final size of epidemic is 50,844 (95% CI: 50757, 50915), and that the total number of hospital patient deaths and total deaths (including those who died due to untimely treatment) are 2920 (95% CI: 2817, 2985), and 5003, (95% CI: 4888, 5065), respectively. Finally, we find that the daily number of new cases becomes zero after April 2, (95% CI: April 2, April 3).

5.2 The number of OW beds in control and curb the epidemic of COVID-19

We perform numerical simulations to illustrate and compare the impact of the number of beds and the timely introduction of OW beds on the transmission dynamics, control and ultimate outcome, of the COVID-19 epidemic in Wuhan.

Fig. 7 shows the number of infected and cumulative deaths if the OW beds are introduced on different dates. The results demonstrate that the sooner the OWs are available, the greater the reduction in the total number of infections, and the shorter the epidemic. If the OWs are activated on January 30, the number of infected will peak on January 31(with a peak value of 12888), and the length of the epidemic will be shortened by 30 days. Compared with the actual situation, the final size of total infection will be decreased by 66%, and the cumulative number of deaths will be reduced by 84%. Furthermore, if the OWs can be activated even earlier on January 23, the epidemic will reach the peak on January 28 with a peak value of only 8976, the final size will decrease by 75%, the epidemic time will be reduced to 36 days, and the cumulative number of deaths will be reduced by 94%. The comparison is also summarized in Table 3.

The timing of putting the beds into use is crucial, it is not just the number of beds available matters, what matters most is when the massively increasing number of confirmed cases need them for complete isolation, there are beds available to keep up the needs. Wuhan planned to build at least 30,000 OW beds[31]. From February 5, when the first OW was launched, to February 22, when newly built beds were no longer needed, a total of 13,348 beds were used. However, if the beds were not constructed and put into use in time to isolate the skyrocketing number of confirmed

cases, the epidemic will become uncontrollable. As shown in Fig. 7(1), we found that if the OWs beds were launched one day later on February 6 (dashed curve), the number of daily new confirmed cases (1967 and 1767 on February 4 and 5 respectively) will infect more people since no more beds available to immediately isolate them, the final size of total infection would reach 7,410,164, the epidemic would become entirely out of control, and it would last for 249 days (dotted curve in Fig. 7(2)). In other words, the 13,348 beds actually used were the minimum number of beds needed to stop the epidemic if the OWs were put into use on February 5.

We now examine the impact of the number OW beds introduced each day on the cumulative number of infections and deaths. Fig. 8 shows the total number of cases (left panel) and cumulative number of deaths (right panel) for different values of $b_2(t)$: 0.8 times, 1.2 times, 1.5 times, and 2 times the actual number of beds used. We find that when the number of beds per day is increased by a factor of 1.2, 1.5, or 2, the peak time of the epidemic will arrive 21, 17 and 16 days earlier with reduced peak values of 29592, 24736 and 21963 infected, respectively. Additionally, we find that the epidemic final size is reduced by 26.4%, 38.1% and 40.7%, that the epidemic lasts for 55, 51 and 48 days, and that the cumulative number of deaths is decreased by 48.7%, 56.38% and 60.34%, respectively.

However, if the number of OW beds per day is reduced by 80% of the actual number used, the epidemic situation will not be effectively controlled (Fig. 8 dashed curve, right panel). The epidemic outcomes will be extreme, since the number of newly built beds is not sufficient for the number of cases needing isolation and treatment. The comparison is summarized in Table 3.

To further explore the key role of OWs in isolating the confirmed cases to stop the epidemic in Wuhan, we simulate to compare two different schedules of using the beds of OWs. If the 13,348 OW beds were put into use within one week with 1964 beds daily, the peak time of the epidemic will be 11 days earlier with peak value of 28,818, and the final size of the total infection will be reduced by 12,952 (52.79% less). Also, the epidemic time will be shortened by 12 days, and the cumulative death will be reduced by 2641. Yet, if the 13,348 OW beds were distributed equally in two weeks with 982 bed daily, it would have missed the window of isolating the large amount of confirmed individuals leading to over 7.4 million total infections. We summarize the comparison simulation results in the last part of Table 3.

Table 3 provides a comparison of the different starting dates, capacities, and introduction schemes of the OW beds. A hospital beds per 1000-infected-person ratio (HBPR) is also listed, determined by the maximum beds used in each simulation. In general, we find that, the earlier the introduction of the OW beds, the smaller the HBPR needed to control the scale of the outbreak (Tables 3 and 4). We also find that if the OW beds are introduced too late, or if the beds are improperly used, the HBPR increases, and does not guarantee effective control of the epidemic (Tables 3 and 4).

5.3 Ratio of hospitalization in the absence of OWs

Before the establishment of the OWs, most patients were requested to be isolated at home due to the lack of medical resources. The contact infection rate among non-HCPs in the model can be used to measure the implementation effect of household quarantine. Next, we analyze the impact of home isolation measures on the prevention and control of the epidemic in the absence of OWs.

In the absence of OWs, the epidemic could still be effectively controlled. Fig. 9 shows that medium to large reductions in contact transmission rates can reduce the peak value of infection and the final size of the epidemic, delay the peak time and reduce the length of the epidemic. However, the total number of deaths may increase. This can be explained by the limitations of DH at the

beginning of the epidemic - insufficient DH resources, and the inability to provide proper care to some critically infected patients. Results are further summarized in Table 5.

In Fig. 10 we show that an increase in the capacity of DHs can also effectively control the epidemic in the absence of OWs. When the number of DHs beds is increased by a factor of 1.5, the peak number of infections is reduced to 13,287, the epidemic final size is reduced to 15,942, the epidemic duration shortened to 29 days, and the number of cumulative deaths is reduced to 1113. In contrast, if the number of DH beds is only 80% of the actual number, the epidemic will spread on a larger scale. These results are further summarized in Table 5.

5.4 Sensitivity analysis

Given the uncertainty of the model parameters, we present a sensitivity analysis of some key model parameters. We employ the well-known *Latin Hypercube Sampling/Partial Rank Correlation Coefficient* (LHS/PRCC) method[40]. The parameters we study are the transmission rates (β's), the proportion of subclinical infections (a) and numbers of DH and OW beds (b_1, b_2). We are interested in understanding how these parameters affect the total asymptomatic and mild/severe symptomatic cases over the epidemic in Phase I, II and III. We generate 3000 samples of the mentioned parameters, using LHS and varying them between 80% and 120% of their estimated values. We then verify the monotonic relationships between the parameters and the models outcomes. PRCC values, which determine the significance (magnitude >0.5 required) of each model parameter to variations in model outcomes are calculated.

We first consider the impact on the subclinical cases in Phase I of the epidemic ($A_{w,h}$). As expected, the parameter related to the proportion of apparent infection has a negative correlation to the output. Indeed, an increment of a will lead to a reduction in the number of individuals in the classes $A_{w,h}$. However, we also observe that parameter b_1 is significantly positively correlated to the subclinical cases in DHs, but significantly negatively correlated to the asymptomatic cases in the general population. This can be understood since the susceptible class in the DHs is replenished by this factor, and if there are not enough beds to hospitalize infectious cases, transmission will increase in the general susceptible population.

In Phase II, as in Phase I, the parameter a is significantly negatively correlated to the subclinical cases. Moreover, we observe that by decreasing the number of beds of OW, the number of subclinical cases in the population increases, reflecting increases in disease spread. This highlights again the importance of building more OW beds to decrease the infection spread. Finally, we observe that A_g is significantly positively correlated to b_2. This is due to the fact that OW HCPs are replenished as a function of this parameter.

5.5 Instantaneous risk indices and assessment considering the impact of hospital beds

Using the formula developed in Section 4, we assess the instantaneous risk of infection in each Phase of the epidemic. Results are shown in Fig. 11. We find that in Phase I, with the increase of the number of beds in DHs (increased in the hospitalization ratio), the risk of transmission is significantly reduced, with an $R(t)< 1$. However, the number of beds was not enough to accept the increasing number of new infections. Although $R(t)$ is less than 1, R_w is still increasing and eventually grows to 0.95. The situation can then worsen, with the risk exceeding 1, if no more beds can be added. When the OWs are put into use with a steadily increasing number of beds in Phase II, R_w drops (Fig. 11, panel 2), however, R_g and R_h increase over time. It manifests that the risk for non-HCPs diminishes as HCP risk increases. Finally, in Phase III, we see that R_w, R_h, and R_g all decrease.

6 Summary and discussion

We have examined the effects of an increasing number of DH and OW beds over three phases of COVID-19 transmission in Wuhan. Our findings show that it was the increasing number of OW beds, used to isolate confirmed infections that eventually controlled the epidemic in Wuhan.

Wuhan was the first severely affected area by the then unknown, novel and deadly SARS-CoV-19 virus. After confirming the risk of human-to-human transmission, China quickly made a decision to inhibit movement from the city.

With the help of people across the country and the world, medical and other resources in Wuhan were supplemented in a timely manner to maintain the function of all hospital beds. At the same time, the building and establishment of DHs, to treat severely affected patients, and OWs, for isolation of mildly infected patients, increased the bed-to-patient ratio in the city thus accelerating the halting of the epidemic. We note that with the increased capacity of hospital beds, increases in healthcare personnel were also likely required to curb this infection.

The lockdown of Wuhan provided a valuable window into the prevention and control of COVID-19 virus in China, and the world[8]. Our studies suggest that, in cities that have implemented social distancing and effective testing rates, but where social conditions may mean that within-home isolation is not sufficient to inhibit transmission, a timely and effective introduction of treatment and isolation beds will be important to curb COVID-19 spread. We therefore strongly suggest that jurisdictions assess the capacity for effective within-home isolation, and where this is not possible, increase the OW type of beds for isolating confirmed cases (i.e., building new hospitals or isolation wards, repurposing government-owned buildings, etc.).

Author Contributions: Research design: H.Z., JuanL, P.Y. B.S., N.O., J.B., J.H., Z.J., J.C., Z.T., M.F.; Data and resources: Y.Y., T.Z., Q.L., P.Y., JuanL.; Modeling: H.Z. and all; Model analysis: JunL., JuanL., Z.J., E.A., H.Z.; Simulations: P.Y., JuanL., T.Z., Y.T., J.D.K.; Draft preparation: JuanL, P.Y., T.Z., Q.L., Y.T., D.D.K., E.A., H.Z.; Writing-reviewing-editing: H.Z., J.H., B.S., N.O., J.B., J.D. K.Supervision: H.Z.

Conflicts of Interest: The authors declare no conflict of interest.

Funding: This research was supported by the Natural Sciences and Engineering Research Council of Canada and York University Research Chair program (HZ).

Reference

1. Timeline of China's fight against the novel coronavirus. China: The State Council of the People's Republic of China; 2020. Available from: http://english.www.gov.cn/news/topnews/202003/19/content_WS5e736ce7c6d0c201c2cbef8f.html [cited Mar 19]
2. Wuhan pulls through the worst, with a tough lockdown. Beijing: National Health Commission of the People's Republic of China; 2020. Available from: http://en.nhc.gov.cn/2020-03/24/c_78142.htm [cited 2020 Mar 24].

3. Entire nation mobilizes to help Wuhan. Beijing: National Health Commission of the People's Republic of China; 2020. Available from: http://en.nhc.gov.cn/2020-03/24/c_78231.htm [cited 2020 Mar 22].

4. The 8th Press Conference of "Prevention and Control of COVID-19". Hubei: Health Commission of Hubei Province; 2020. Available from: http://wjw.hubei.gov.cn/fbjd/dtyw/202001/t20200130_2016544.shtml [cited 2020 Mar 3].

5. Leishen Hospital begins to treat patients. Hubei: Health Commission of Hubei Province. Available from: http://wjw.hubei.gov.cn/bmdt/ztzl/fkxxgzbdgrfyyq/fkdt/202002/t20200210_2022622.shtml [cited 2020 Feb 29].

6. Update information on the novel coronavirus in Hubei on February 3, 2020. Wuhan: Wuhan Municipal Health Commission; 2020. Available from: http://wjw.hubei.gov.cn/fbjd/tzgg/202002/t20200204_2018743.shtml [cited 2020 Feb 4].

7. First batch of "square cabin hospitals" was officially opened. China: Central People's Government of the People's Republic of China; 2020. Available from: http://www.gov.cn/xinwen/2020-02/06/content_5475062.htm [cited 2020 Feb 6].

8. Report of the WHO-China Joint Mission on Coronavirus Disease 2019 (COVID-19). Geneva: World Health Organization; 2020. Available from: https://www.who.int/docs/default-source/coronaviruse/who-china-joint-mission-on-covid-19-final-report.pdf. [cited 2020 Mar 30]

9. The transcript of the press conference on February 4, 2020. Beijing: National Health Commission of the People's Republic of China; 2020. Available from: http://www.nhc.gov.cn/wjw/xwdt/202002/35990d56cfcb43f4a70d7f9703b113c0.shtml [cited 2020 Feb 4].

10. Wuhan: Wuhan Municipal People's Government; 2020. Available from: http://wjw.wuhan.gov.cn/front/web/showDetail/2020021509592 [cited 2020 Feb 15].

11. Epidemiology Working Group for NCIP Epidemic Response. The epidemiological characteristics of an outbreak of 2019 novel coronavirus diseases (COVID-19) in China. *Chinese Journal of Epidemiology*. 2020 02 17; 41(2):145-151. doi: http://doi.org/10.3760/cma.j.issn.0254-6450.2020.02.003.PMID:32064853

12. Wu JT, Leung K, Leung GM. Nowcasting and forecasting the potential domestic and international spread of the 2019-nCoV outbreak originating in Wuhan, China: a modelling study. *Lacent*. 2020 02 29; 395(10225): 689-697. doi: https://doi.org/10.1016/S0140-6736(20)30260-9.PMID:32014114

13. Tang B, Wang X, Li Q, Nicola LB, Tang SY, Xiao YN, Wu JH. Estimation of the Transmission Risk of the 2019-nCoV and Its Implication for Public Health Interventions. *J Clin Med*. 2020 02 07; 9(2): 462. doi: https://doi.org/10.3390/jcm9020462.PMID:32046137

14. Wang HW, Wang ZZ, Dong YQ, Chang RJ, Xu C, Yu XY, et al. Phase-adjusted estimation of the number of Coronavirus Disease 2019 cases in Wuhan, China. *Cell Discov*. 2020 02 24; 6: 10. doi: https://doi.org/10.1038/s41421-020-0148-0.PMID:32133152

15. Chen TM, Rui J, Wang QP, Zhao ZY, Cui JA, Yin L. A mathematical model for simulating the phase-based transmissibility of a novel coronavirus. *Infect Dis Poverty*. 2020 02 28; 9(1):24 . doi: https://doi.org/10.1186/s40249-020-00640-3.PMID:32111262

16. WHO Director-General's opening remarks at the media briefing on COVID-19 - 11 March 2020. Geneva: World Health Organization; 2020. Available from: https://www.who.int/dg/speeches/detail/who-director-general-s-opening-remarks-at-the-media-briefing-on-covid-19---11-march-2020 [cited 2020 Mar 11].

17. Spanish Prime Minister Announced National Shutdowns. Washington, D.C.: The HILL; 2020. Available from: https://thehill.com/policy/international/487605-spain-announces-lockdown-over-coronavirus [cited 2020 Mar 15].

18. Italy was starting to shut down on March 10th. Available from: https://en.wikipedia.org/wiki/2020_Italy_coronavirus_lockdown [cited 2020 Mar 20].

19. San Francisco announces three week lockdown: Residents are BANNED from leaving home after midnight on Tuesday for anything but doctor's visits or grocery shops to fight coronavirus. London: Daily Mail News; 2020. Available from: https://www.dailymail.co.uk/news/article-8118417/San-Francisco-announces-three-week-lockdown.html [cited 2020 Mar 21].

20. COVID-19: Vancouver closes all restaurants, playgrounds. Vancouver: Vancouver Sun News; 2020. Available from: https://vancouversun.com/news/covid-19-vancouver-closes-all-restaurants-playgrounds/ [cited 2020 Mar 20].

21. Epidemic situation of COVID - 19 in Wuhan city. Wuhan: Wuhan Municipal Health Commission (WMHC); 2020. Available from: http://wjw.wuhan.gov.cn/front/web/showDetail/2020031610125 [cited 2020 Mar 16]

22. Wuhan Municipal Health Commission (WMHC). Available from: http://wjw.wuhan.gov.cn/front/web/list3rd/no/803 [cited 2020 Mar 21]

23. Notice concerning the issuance of a protocol for the diagnosis and treatment of COVID-19. China: Central People's Government of the People's Republic of China; 2020. Available from: http://www.gov.cn/zhengce/zhengceku/2020-02/05/content_5474791.htm [cited 2020 Feb 27].

24. Wang DW, Hu B, Hu C, et al. Clinical Characteristics of 138 Hospitalized Patients With 2019 Novel Coronavirus–Infected Pneumonia in Wuhan, China. *JAMA-J Am Med Assoc*. 2020 02 07. doi: https://doi.org/10.1001/jama.2020.1585. PMID:32031570

25. Li Q, Guan X, Wu P, et al. Early Transmission Dynamics in Wuhan, China, of Novel Coronavirus–Infected Pneumonia. *N Engl J Med*. 2020 03 26; 382(13): 1199-1207. doi: http://doi.org/10.1056/NEJMoa2001316.PMID:31995857

26. Report of Wuhan Hospital Quarantine Area. Available from: https://www.yicai.com/news/100498867.html [cited2020 Feb 20].

27. The use of hospital beds in designated hospitals in the city. Wuhan: Wuhan Municipal Health Commission; 2020. Available from: http://wjw.wuhan.gov.cn/front/web/showDetail/2020020209322 [cited 2020 Feb 2].

28. The last square cabin hospital is closed. The square cabin hospital successfully completed its historical mission**.** China: National Health Commission of the People's Republic of China; 2020. Available from: https://m.chinanews.com/wap/detail/zw/sh/2020/03-11/9121442.shtml [cited 2020 Mar 11].

29. Facilities report more empty beds as a result of discharges. Beijing: The State Council of the People's Republic of China; 2020. Available from: http://english.www.gov.cn/news/topnews/202003/04/content_WS5e5efd7fc6d0c201c2cbd78b.html [cited Mar 14].

30. 14 temporary hospitals closed in China's Wuhan as more patients discharged. Beijing: The State Council of the People's Republic of China; 2020. Available from: http://english.www.gov.cn/news/photos/202003/10/content_WS5e66d23cc6d0c201c2cbdea8.html [cited Mar 14].

31. The 29th Press Conference of "Prevention and Control of COVID-19". Hubei: Health Commission of Hubei Province; 2020. Available from:

http://wjw.hubei.gov.cn/bmdt/ztzl/fkxxgzbdgrfyyq/xxfb/202002/t20200222_2145206.shtml [cited 2020 Feb 23].

32. Bao LL, Deng W, Gao H, Xiao C, et al. Reinfection could not occur in SARS-CoV-2 infected rhesus macaques. *BioRxiv*. 2020 03 14. doi: https://doi.org/10.1101/2020.03.13.990226.

33. Van den Driessche P, Watmough J. Reproduction numbers and sub-threshold endemic equilibria for compartmental models of disease transmission. *Math Biosci*. 2002 11; 180: 29-48. doi: http://doi.org/10.1016/S0025-5564(02)00108-6. PMID:12387915

34. Heffernan JM, Smith RJ, Wahl LM. Perspectives on the basic reproductive ratio. *J R Soc Interface*. 2005 09 22; 2(4): 281–293.doi:https://doi.org/10.1098/rsif.2005.0042 PMID:16849186

35. Webb GF, Blaser MJ, Zhu H, Ardal S, Wu J. Critical Role of Nosocomial Transmission in the Toronto SARS Outbreak. *Math Biosci Eng*. 2004 03 01; 1(1): 1–13. doi: https://doi.org/10.3934/mbe.2004.1.1 PMID:20369956

36. Busenberg S, Cooke K. Vertically Transmitted Diseases. Springer-Verlag, New York, 1993.

37. Brauer F, Castillo-Chavez C. Mathematical Models in Population Biology and Epidemics. Springer-Verlag, New York, 2000.

38. Hethcote HW. The mathematics of infectious diseases. *SIAM Rev*. 2000; 42(4): 599–653. doi: https://doi.org/10.1137/S0036144500371907

39. Haario H, Laine M, Mira A, Saksman E. *DRAM: Efficient adaptive MCMC*. Stat Comput 16. 2006 11; 339-354. doi: http://doi.org/10.1007/s11222-006-9438-0.

40. Mckay MD, Beckman RJ, Conover WJ. Comparison of 3 Methods for Selecting Values of Input Variables in the Analysis of Output from a Computer Code. *Technometrics.* 1979; 21(2): 239–245. doi: https://doi.org/10.1080/00401706.1979.10489755

41. The transcript of the press conference on February 28, 2020. Beijing: National Health Commission of the People's Republic of China; 2020. Available from: http://www.nhc.gov.cn/xcs/s3574/202002/2fb820181d8a41969bca041793c11bcb.shtml [cited 2020 Mar 8].

42. Li RY, Pei S, Chen B, Song YM, Zhang T, Yang W, Shaman J. Substantial undocumented infection facilitates the rapid dissemination of novel coronavirus (SARS-CoV2). *Science*. 2020 03 16. doi: http://doi.org/10.1126/science.abb3221.PMID:32179701

43. 2% to 5% of mild patients in cabin hospitals convert to severe patients. Available from: http://www.bjd.com.cn/a/202002/19/WS5e4d4683e4b0094948681f15.html [cited 2020 Feb 19].

44. Press conference on the work of epidemic prevention and control. China: Central People's Government of the People's Republic of China; 2020. Available from: http://www.gov.cn/xinwen/2020-02/20/content_5481420.htm#1 [cited 2020 Mar 11].

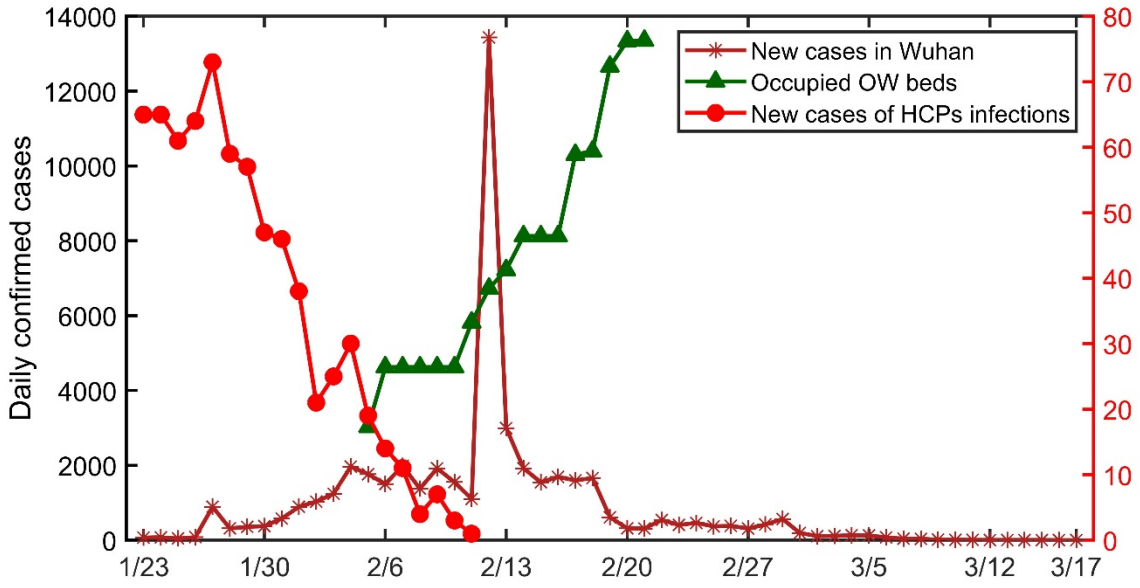

Figure 1. Daily reported confirmed cases of COVID-19 in Wuhan from January 23 to March 17, 2020 (blue). The cumulative number of daily occupied hospital beds in OWs from February 5 to 22 (green) and the daily new confirmed cases of HCPs from January 23 to February 11, 2020 (red) are also shown. Data sources: Wuhan Municipal Health Commission (WMHC)[22].

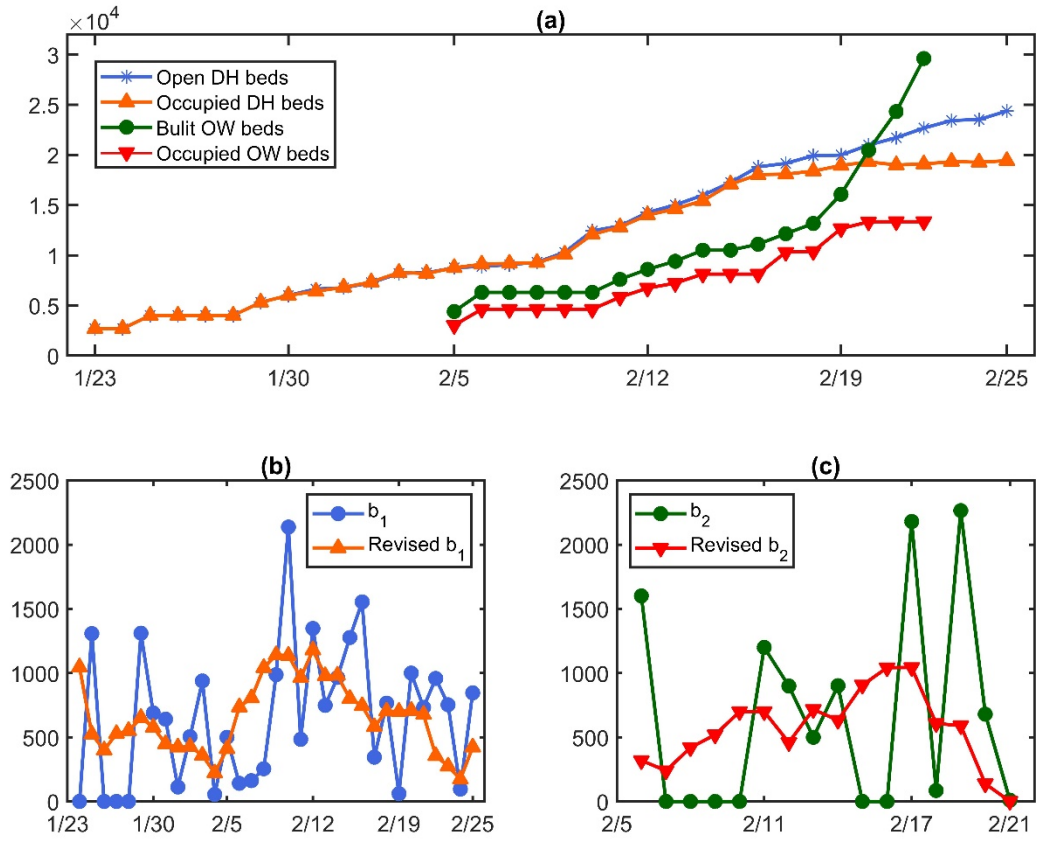

Figure 2. The cumulative number of open beds in OWs and DHs and the planned number of beds in OWs. (a). Open and occupied beds in DHs and OWs. (b). Daily new beds available in DHs. (c). Daily new beds available in OWs. Data source[41].

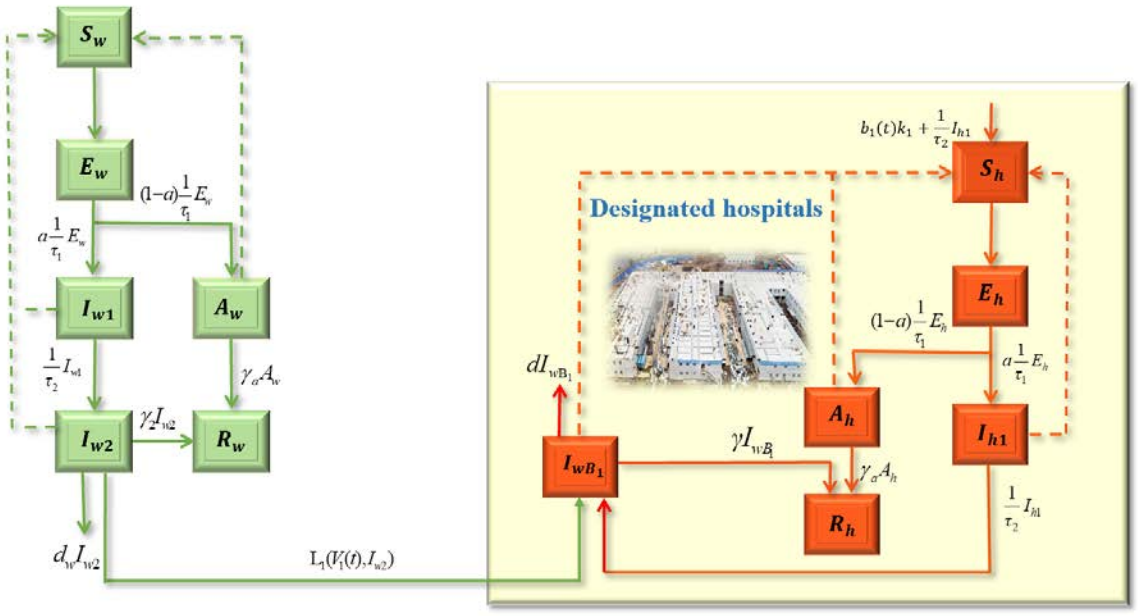

Figure 3. Schematic representation of the dynamics of COVID-19 in Wuhan for Phase I, from January 23 to February 5 (the period when only DHs were used to treat severe cases). Solid lines indicate the movement between classes. Dashed lines represent the virus transmission routes.

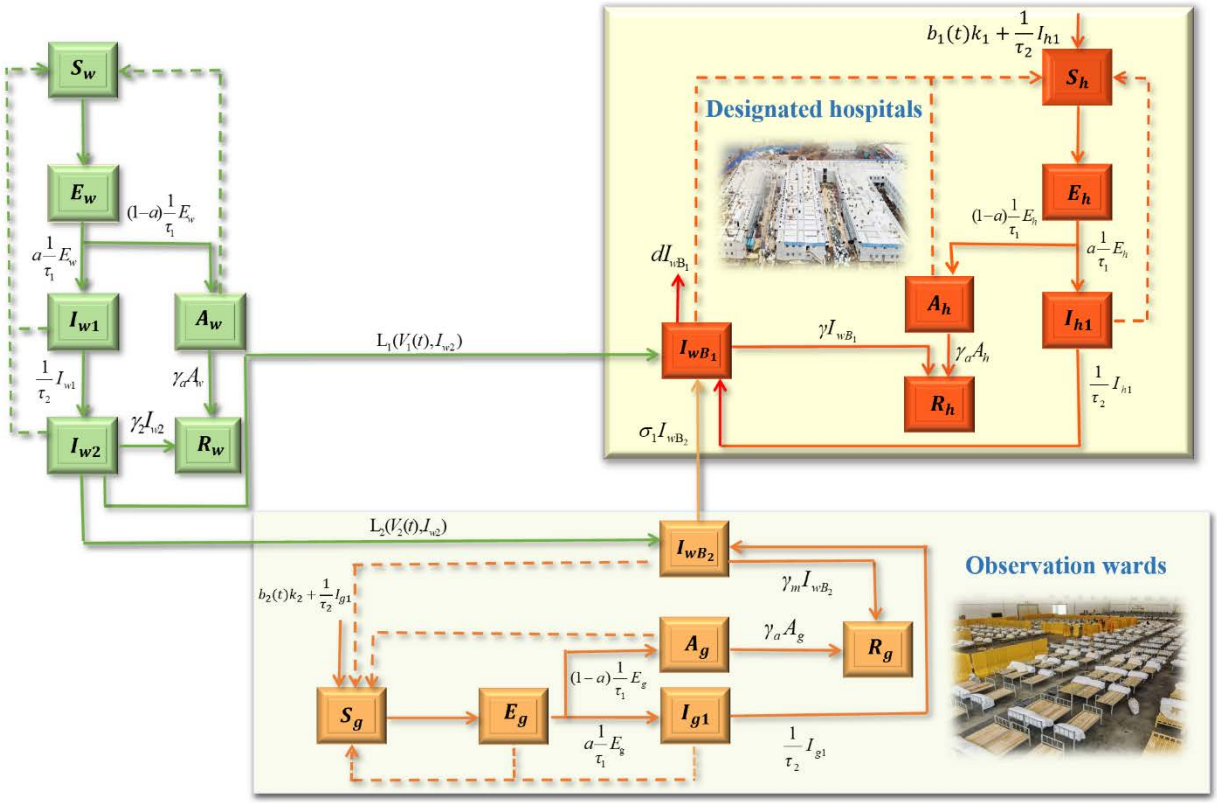

Figure 4. Schematic representation of the dynamics of COVID-19 in Wuhan in Phase II, from February 5 to February 22 (the period when the increasing number of beds in OWs were used to house infected with mild symptoms). Solid lines indicate population movement. Dashed lines represent the virus transmission routes.

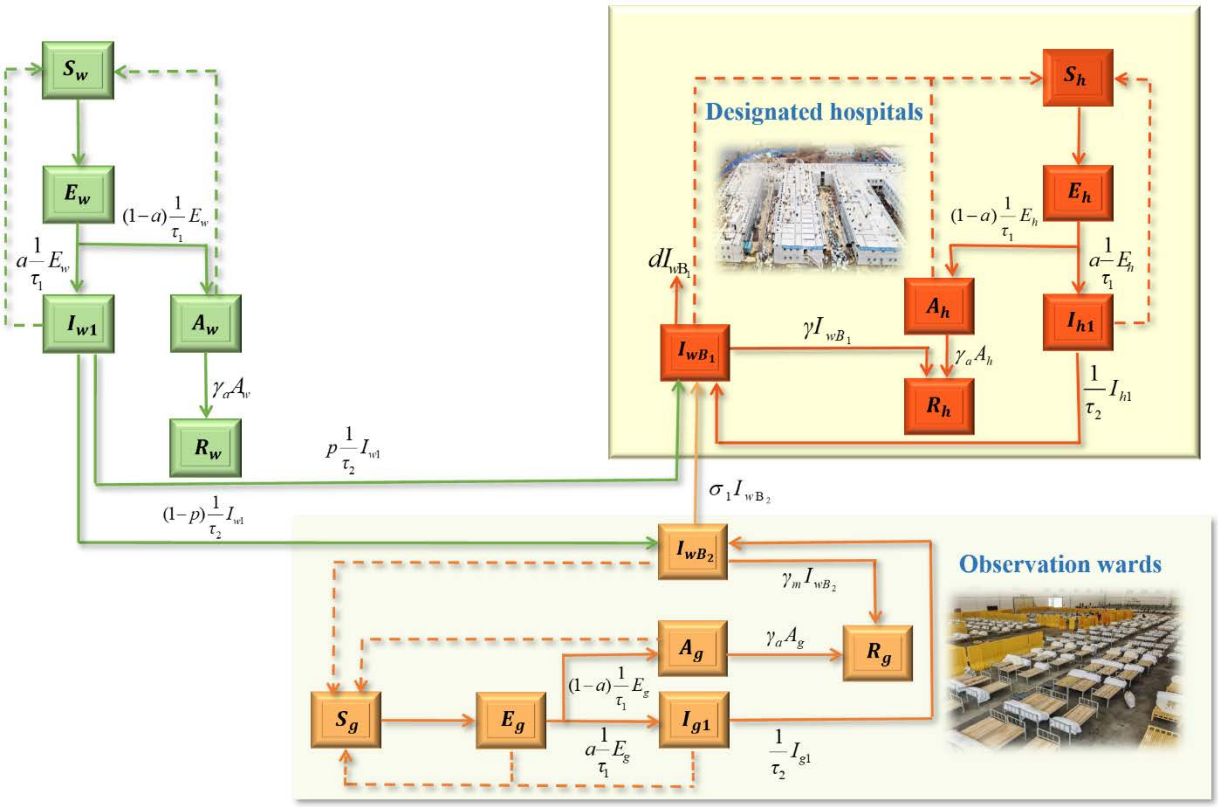

Figure 5. Schematic representation of the dynamics of COVID-19 in Wuhan for Phase III, from February 22 till the end of the outbreak (the period when both DHs and OWs have more and more used beds remained empty). Solid lines indicate the movement of the involving population. Dash lines represent the virus infection actions.

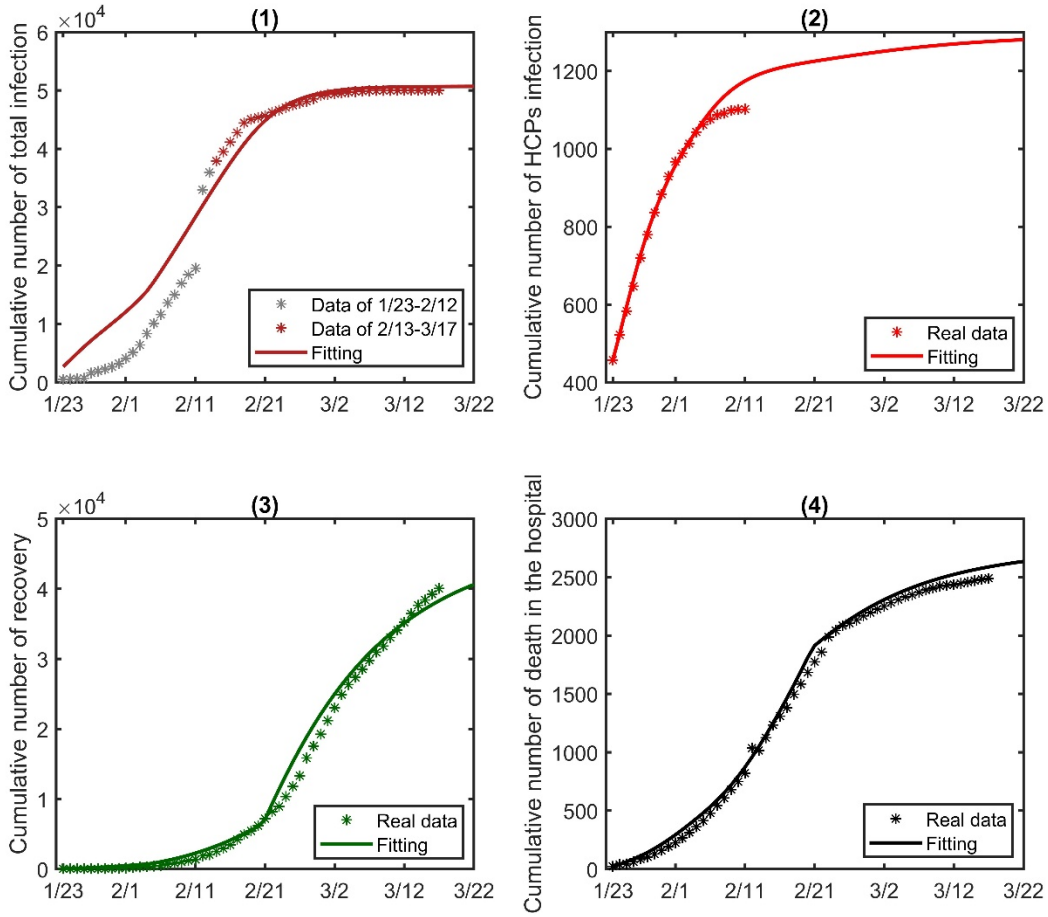

Figure 6. Data fitting for selected epidemic outcomes of COVID-19 in Wuhan form January 23 to March 17, 2020, including Phases I-III: (1) the cumulative number of confirmed cases, (2) the cumulative number of HCPs confirmed cases (3) the cumulative number of recovered, (4) the cumulative number of deaths. Circles represent real data; solid curves depict model fits. The data from January 23 to February 12 (grey star markers) are not used in the parameter estimation (see Section Data and Materials).

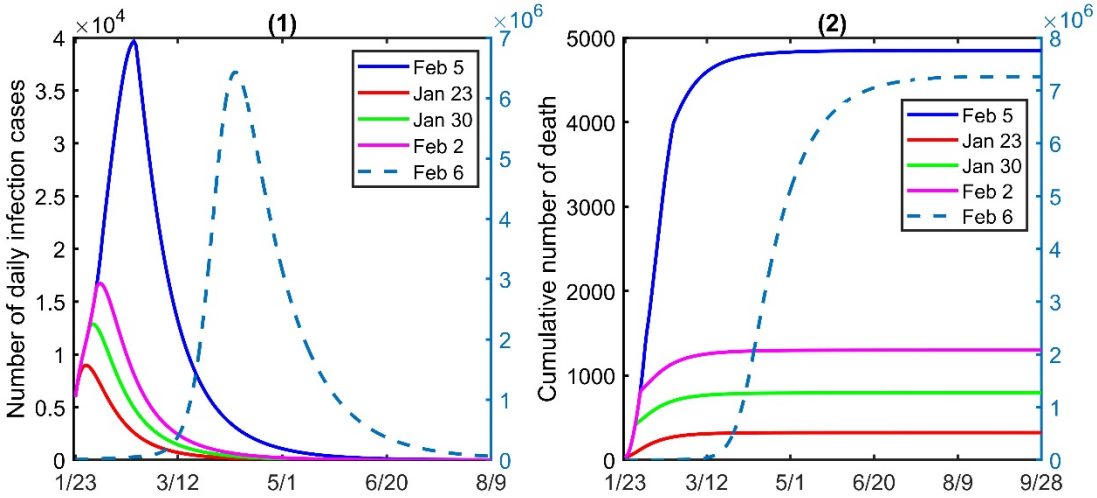

Figure 7. Illustration of what would have happened had the OWs be put into use on different dates: February 5 (blue, the real situation), January 23 (red), January 30 (green), February 2 (magenta), and February 6 (Light blue dashed curve, with the vertical axis on the right). Panel (1) is the number of infected, and Panel (2) the cumulative number of deaths.

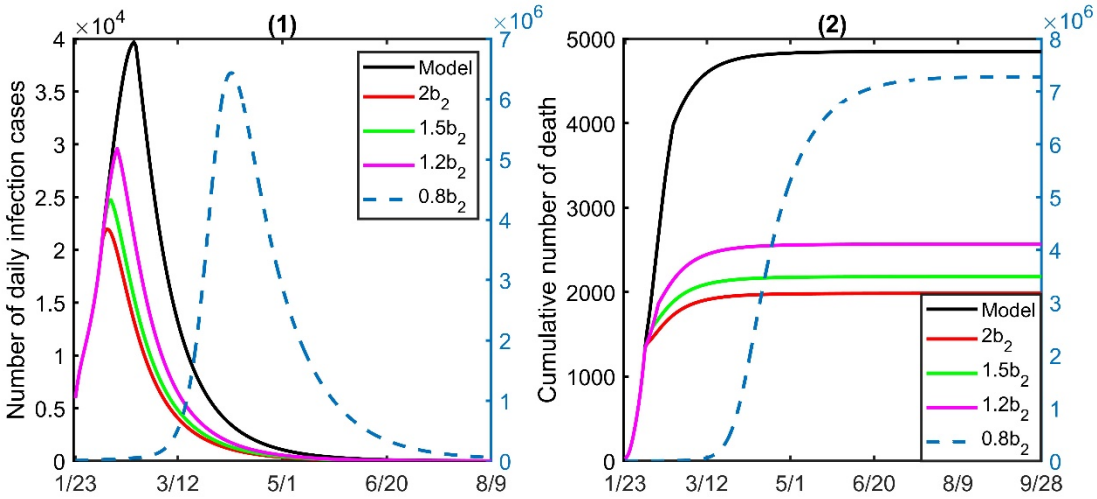

Figure 8. Comparison of the effect of different number of OW beds put into use on February 5. The black curve is from model fitting; compared with 2 times (red), 1.5 times (green), 1.2 times (magenta) and 0.8 times (dashed) the number of OW beds actually used: (1) the number of daily infections, (2) the cumulative number of total deaths.

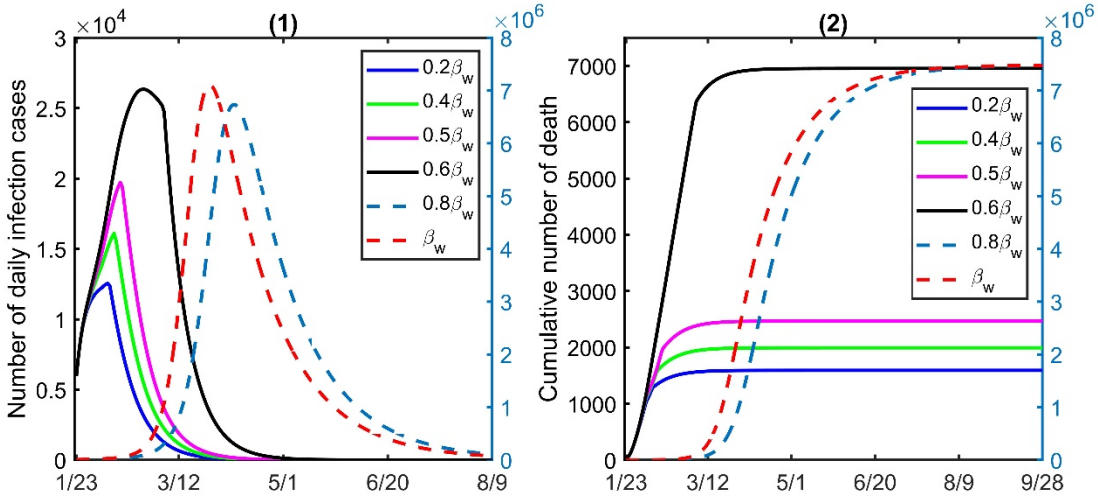

Figure 9. Comparison between different contact transmission rate in the absence of OWs. $0.2\beta_w$ (blue solid) , $0.4\beta_w$ (green), $0.5\beta_w$ (magenta) and $0.6\beta_w$ (black), $0.8\beta_w$ (light blue) and β_w (red), where $\beta_w = (\beta_{w1}, \beta_{w2})$; Panel (1) is the number of daily infections, Panel (2) the cumulative number of deaths.

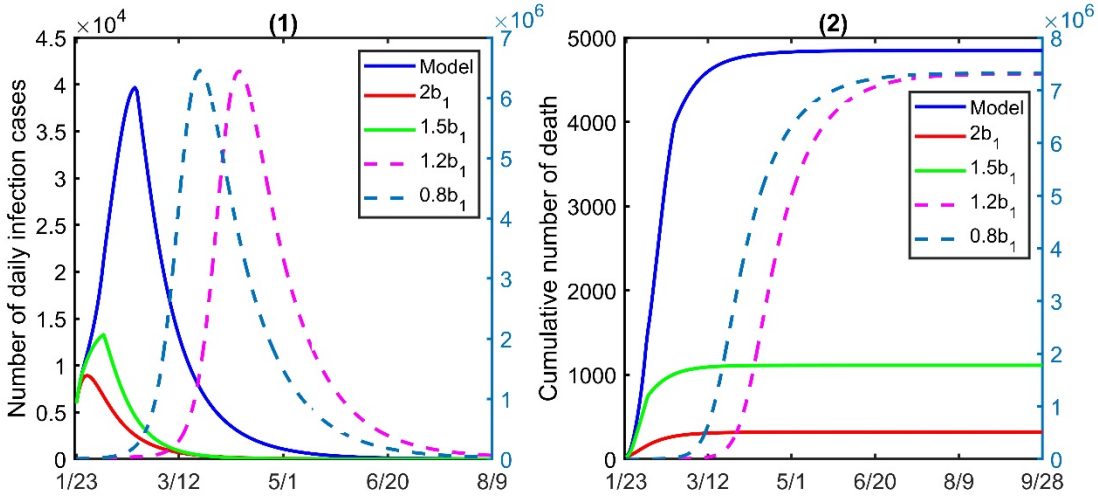

Figure 10. Impact of hospitalization ratio on the cumulative number of infections and deaths over time with different number of DH beds in the absence of OWs.

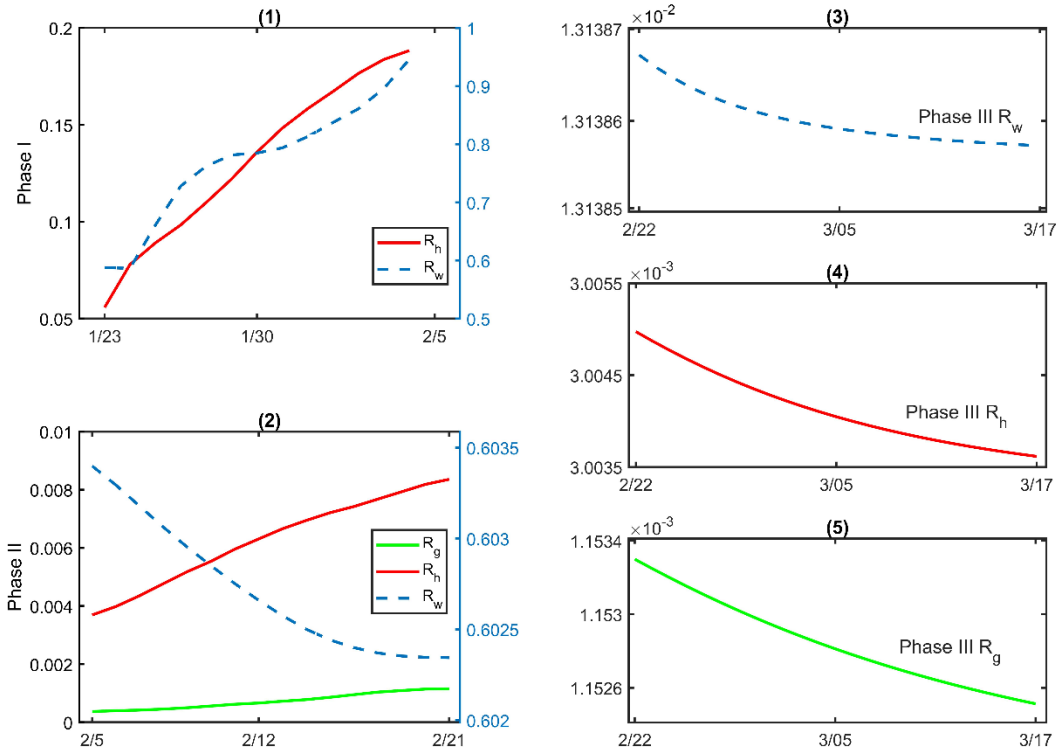

Figure 11. The instantaneous risk indices for general population, HCPs in DHs and OWs over the three phases. General population (light blue curve, right panel), HCPs in DHs (red) and HCPs in OWs (green). Phase I (1); Phase II (2); and Phase III (3), (4) and (5).

Tables

Table 1. Identification of the variables and their initial values

Variables	Descriptions	Initial Values	95% CI[a]	Sources
$S_w(t)$	Number of susceptible non-HCPs	1.1060e+07	(1.1060e+07, 1.1060e+07)	MCMC[b]
$E_w(t)$	Number of exposed non-HCPs	6667.5	(6600.7, 6750.9)	MCMC
$A_w(t)$	Number of inapparent infected non-HCPs (that will never develop symptoms)	13.758	(13.589, 14.002)	MCMC
$I_{w1}(t)$	Number of infected non-HCPs without symptoms that will become symptomatic	2956.4	(2944.8, 2967.5)	MCMC
$I_{w2}(t)$	Number of infected and untreated non-HCPs with symptoms	115.01	(113.92, 115.83)	MCMC
$R_w(t)$	Number of recovereds non-HCPs out of hospitals	1.5833	(1.5664, 1.6033)	MCMC
$S_h(t)$	Number of susceptible HCPs that work in DHs	6692	-	Calculated[c]
$E_h(t)$	Number of exposed HCPs that work in DHs	426	-	Calculated[d]
$A_h(t)$	Number of inapparent (subclinical) infected HCPs that work in DHs, will never show symptoms	2	-	22[e]
$I_{h1}(t)$	Number of infected HCPs that work in DHs that do not symptoms that will become symptomatic	190	-	Calculated[f]
$R_h(t)$	Number of recovered patients from DHs	31	-	22
$I_{wB_1}(t)$	Total number of patients in DHs	2692	-	22
$S_g(t)$	Number of susceptible HCPs that work in OWs	0	-	
$E_g(t)$	Number of exposed HCPs that work in OWs	0	-	
$A_g(t)$	Number of inapparent infected HCPs that work in OWs, that will never show symptoms	0	-	
$I_{g1}(t)$	Number of infected HCPs that work in OWs that do not show symptoms that will become symptomatic	0	-	
$R_g(t)$	Number of recovered patients from OWs	0	-	
$I_{wB_2}(t)$	Total number of patients in OWs	0	-	

Note: a) 95% CI: 95% highest posterior density interval; b) MCMC：Markov Chain Monte Carlo; c) Calculated by multiplying the initial beds in DHs by k_1; d) Calculated by summing the HCPs infection cases in the first seven days (incubation period, $\tau_1 + \tau_2$); f) Calculated by summing the HCPs infection cases in the first three days (τ_2).

Table 2. Parameter estimation for COVID-2019 in Wuhan, China

Parameters	Descriptions	Estimated Mean Values	95% CI[a]	Sources
β_{w1}	Infection rate of susceptible non-HCPs by non-HCP infectious individuals without symptoms.	3.3775e-10	(3.3391e-10, 3.4015e-10)	MCMC[b]
β_{w2}	Infection rate of susceptible non-HCPs by non-HCP infectious symptomatic individuals that are not in DHs or OWs.	5.4667e-08	(5.4304e-08, 5.5022e-08)	MCMC
β_h[c]	Infection rate of susceptible HCPs in DHs by infectious patients	I: 1.2477e-07 II-III: 1.6699e-09	(1.2425e-07, 1.2527e-07) (1.6570e-09, 1.6814e-09)	MCMC
β_{h1}[d]	Infection rate of susceptible HCPs in DHs from infectious asymptomatic DH HCPs.	I: 7.0175e-09 II-III: 9.5218e-10	(6.8941e-09, 7.1492e-09) (9.2651e-10, 9.6620e-10)	MCMC
β_g	Infection rate of susceptible HCPs in MHs by infectious patients.	3.3342e-09	(3.3104e-09, 3.3573e-09)	MCMC
β_{g1}	Infection of susceptible HCPs in OWs from infectious asymptomatic OW HCPs.	1.6957e-09	(1.6374e-09, 1.7261e-09)	MCMC
γ_a	Recovery rate of inapparent infected	0.0700	(0.06929, 0.0708)	MCMC
γ_2	Recovery rate of infected and untreated non-HCPs with symptoms.	0.0133	(0.01306, 0.0134)	MCMC
γ[e]	Recovery rate of patients in DHs.	I-II: 0.0089 III: 0.0839	(0.0088, 0.0090) (0.0829, 0.0846)	MCMC
γ_m	Recovery rate of patients in OWs.	0.0241	(0.0238, 0.0247)	MCMC
d_w	Disease-induced death rate of infected and untreated non-HCPs with symptoms.	0.0306	(0.0304, 0.0308)	MCMC
d[e]	Disease-induced death rate in DHs.	I-II: 0.0054 III: 0.0022	(0.0051, 0.0056) (2.1587e-03, 2.2099e-03)	MCMC
a	The proportion of infecteds with apparent infection	0.9530	(0.9502, 0.9560)	MCMC
p	Fraction of patients admitted into DHs after T_2.	0.7802	(0.7763, 0.7853)	MCMC
τ_1	Average time spent in the exposed classes, E_w, E_h, E_g.	4	-	42
τ_2	Average time period spent in I_{w1}, I_{h1}, I_{g1}.	3	-	42
k_1[f]	Bed to HCP ratio in DHs.	2.486	-	26, 27
k_2[f]	Bed to HCP ratio in OWs.	1.107	-	28
σ_1	The transfer rate of patients from OWs to DHs.	0.02	-	43

Note: a) 95% CI: 95% highest posterior density interval; b) MCMC Markov Chain Monte Carlo; c) The infection rate of susceptible HCPs in DHs by infectious patients in stage I is different from that in stages II and III (due to the strict measures put in place to protect HCPs after the first stage[44]). d) Because of the strict measures put in place to protect HCPs, Infection rate of susceptible HCPs in DHs from infectious asymptomatic DH HCPs in Phase II and III are also different from that in Phase I. e) In Phase III, the recovery and death rates in DHs are different from those in Phase I and II, because the hospital beds are sufficient. f) The ratio of hospital beds to DH and OW HCPs is calculated using the data in reference[26-28].

Table 3. Prevalence values under different OWs usages

	Peak size	Peak time (days)	Final size of infections	Epidemic time (days)	Final size of death	HBPR
3 phases models	39771	30	50844	71	5003	3.323
Without OWs	6450554	64	7386643	242	7318754	2.200
Different date to start using OWs						
Jan.23	8976	6	12729	35	324	0.625
Jan.30	12888	9	17218	41	795	0.931
Feb.2	16736	13	22606	47	1301	1.224
Feb. 6	6429774	78	7410164	249	7264335	3.411
Using different number of OWs beds						
$2b_2(t)$	21963	16	30164	53	1984	1.613
$1.5b_2(t)$	29592	21	37426	60	2566	2.282
$1.2b_2(t)$	24736	17	31491	54	2182	1.860
$0.8b_2(t)$	6433106	76	7405419	247	7275621	3.141
Using the 13348 OW beds in one or two weeks						
1964 beds daily	28818	19	37892	59	2362	2.138
982 beds daily	6432490	76	7409716	247	7265467	3.411

Table 4. Prevalence values if OWs were put into use on February 6

	Peak size	Peak time (days)	Final size of infections	Epidemic time (days)	Final size of death	HBPR
Feb. 6	6429774	78	7410164	249	7264335	3.411
OW 1.2*b2	37497	26	48836	68	4290	2.976
Feb 7,+2500	33610	23	42282	63	3053	2.632
Feb 9,+2500	36468	25	46747	67	4064	2.893
Feb 12,+2500	41609	28	54116	72	4893	3.345

Table 5. Prevalence values without using OWs

	Peak size	Peak time (days)	Final size of infections	Epidemic time (days)	Final size of death	HBPR
3 phases models	39771	30	50844	71	5003	3.323
Without OWs	6450554	64	7386643	242	7318754	2.200
Different contact infection rate						
$0.2\beta_w$	12550	16	15026	40	1592	1.036
$0.4\beta_w$	16094	19	19947	46	1992	1.277
$0.5\beta_w$	19718	22	24679	51	2468	1.573
$0.6\beta_w$	26344	33	37002	68	6954	2.197
$0.8\beta_w$	6732956	76	7550327	277	7474610	2.181
β_w	7103644	65	7548561	266	7476108	2.180
Different number of DH beds put into use						
$2b_1$	8924	6	12721	35	321	0.621
$1.5b_1$	13287	14	15942	42	1113	1.068
$1.2b_1$	6444154	79	7393293	257	7311100	2.536
$0.8b_1$	6453100	60	7380533	238	7326132	1.732